Liquid Crystals

Publication details, including instructions for authors and subscription information:
http://www.informaworld.com/smpp/title~content=t713926090

Chiral banana liquid crystals derived from sugars

G. Gesekus[a]; I. Dierking Corresponding author[b]; S. Gerber[a]; M. Wulf[a]; V. Vill[a]
[a] Institut für Organische Chemie, Universität Hamburg, D-20146 Hamburg, Germany [b] Department of Physics and Astronomy, Schuster Laboratory, University of Manchester, Manchester M13 9PL, UK

To cite this Article Gesekus, G. , Dierking Corresponding author, I. , Gerber, S. , Wulf, M. and Vill, V.(2004) 'Chiral banana liquid crystals derived from sugars', Liquid Crystals, 31: 2, 145 — 152

To link to this Article: DOI: 10.1080/02678290310001639616

URL: http://dx.doi.org/10.1080/02678290310001639616

LIQUID CRYSTALS, VOL. 31, NO. 2, FEBRUARY 2004, 145–152

Chiral banana liquid crystals derived from sugars

G. GESEKUS, I. DIERKING†*, S. GERBER, M. WULF and V. VILL
Institut für Organische Chemie, Universität Hamburg, Martin-Luther-King-Platz 6,
D-20146 Hamburg, Germany
†Department of Physics and Astronomy, Schuster Laboratory, University of
Manchester, Oxford Road, Manchester M13 9PL, UK

(*Received 18 August 2003; accepted 4 October 2003*)

This paper describes the synthesis and physical properties of a chiral bent-core liquid crystal containing the chiral non-aromatic central ring system 1,5-anhydro-2-desoxy-D-*arabino*-hexitol. The preparation involved a stepwise construction of the mesogenic side chains via a selective diesterification of glucal at positions three and six with 4-*O*-acetylbenzoyl chloride followed by selective deacetylation. Repeated esterification of the aromatic hydroxy group with a substituted benzoic acid and hydrogenation of the double bond resulted in the desired product. To our knowledge, this is the first banana shaped liquid crystal synthesized containing a sugar derivative as a chiral core. Investigation of the mesogenic properties and electro-optic experiments showed traditional calamitic phases along with banana phases.

1. Introduction

It had long been thought that for symmetry reasons only chiral molecules may form liquid crystalline phases with polar properties, such as ferroelectricity [1]. Only recently it was demonstrated that the steric packing of bent-core mesogens can induce polar order and a chirality of smectic layers, despite the fact that the constituent molecules are achiral [2]. Since the first bent-core or so called 'banana'-mesogens were characterized in more detail, it has become apparent, that these molecules exhibit novel liquid crystalline phases with unusual properties, and are qualitatively different from traditional calamitic phases [3]. In particular, the occurrence of polar switching in phases composed of achiral molecules has attracted considerable interest in recent years. The reported switching process was first thought to be of ferroelectric nature [2], but has later been shown to be antiferroelectric [4]. To date, several different banana-phases have been identified, some of which are switchable and others, which appear to be of higher order, comparable to crystalline smectics. An overview of bent-core compounds, their phases and properties can be found elsewhere [3].

In this paper we report the synthesis, characterization and physical properties of the first bent-core mesogen with a chiral carbohydrate based central bent unit, which exhibits traditional calamitic phases along with banana phases.

2. Experimental

The compound under investigation is a chiral bent-core mesogen with the structural formula given in figure 1.

Its preparation resulted from our interest in the specific synthesis of chiral dopants exhibiting high helical twisting powers in cholesteric mixtures, which led us to the preparation of the 1,5-anhydro-2-desoxy-D-*arabino*-hexitol (compound **6**) according to the procedure shown in figure 2. Deacetylation of the commercially available starting material 3,4,6-*tri*-*O*-acetyl-D-glucal (**1**) gave deprotected D-glucal (**2**). For the mesogenic side chains consisting of two extended benzoyl groups we chose a stepwise assembly. A direct and convenient entry to 3,6-disubstituted glucal derivatives is given by the method of Guthrie *et al.* [5]. Thus, selective benzoylation of the hydroxyl groups at positions 3 and 6 of D-glucal using benzoyl chloride in pyridine as solvent can be achieved in good yields. After diacylation of compound **2** using 4-*O*-acetylbenzoyl chloride, a selective deacetylation of the

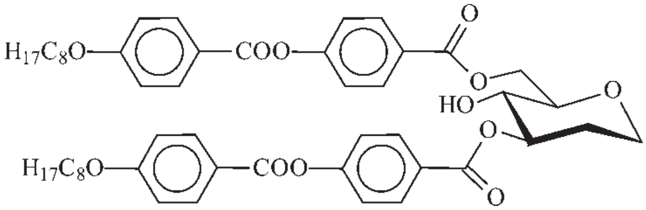

Figure 1. 1,5-Anhydro-2-desoxy-D-*arabino*-hexitol derivative **6**.

---

*Author for correspondence; e-mail: dierking@reynolds.ph.man.ac.uk

Liquid Crystals ISSN 0267-8292 print/ISSN 1366-5855 online © 2004 Taylor & Francis Ltd
http://www.tandf.co.uk/journals
DOI: 10.1080/02678290310001639616

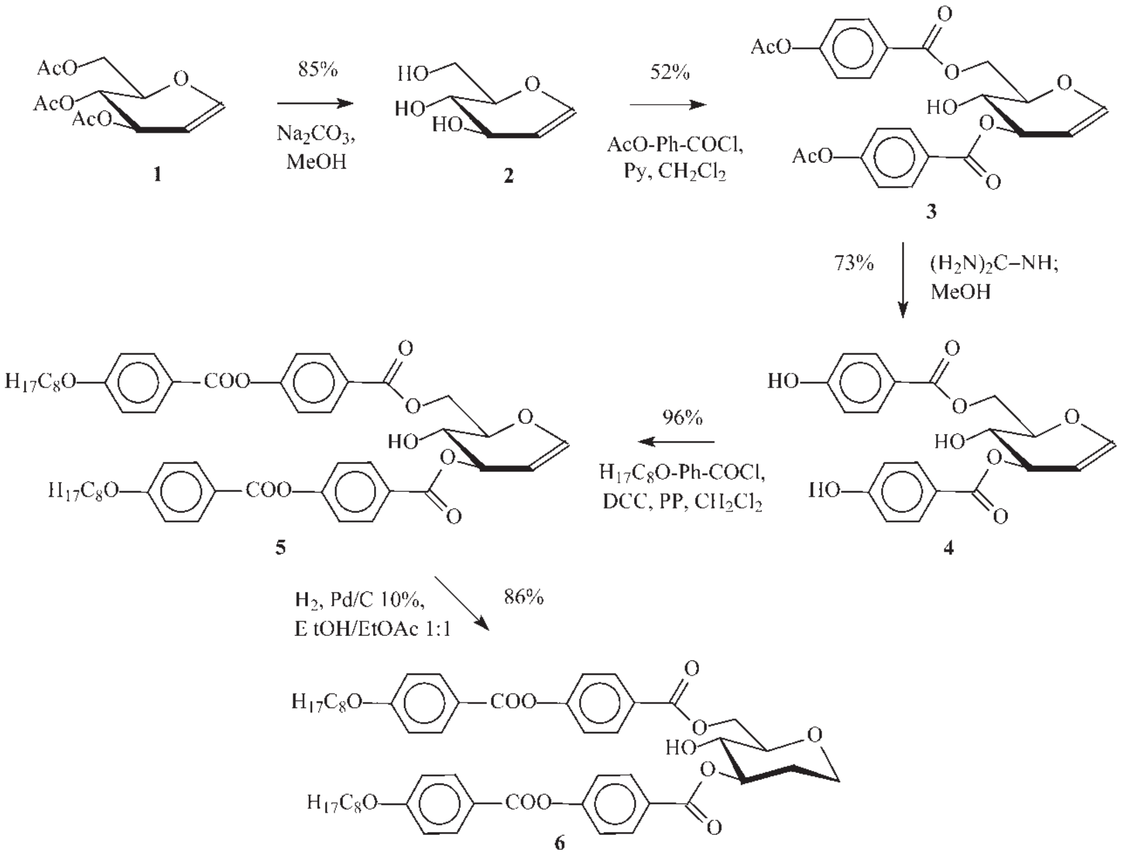

Figure 2. Synthesis of compound **6**.

aromatic *O*-acetyl groups of compound **3** was achieved via a modification of a method described by Kunesch *et al.* [6], using guanidine as deacetylating agent. This smooth deacetylation was followed by selective DCC esterification of the aromatic hydroxy groups leaving the OH group of the alkyl ring intact. In a last reaction

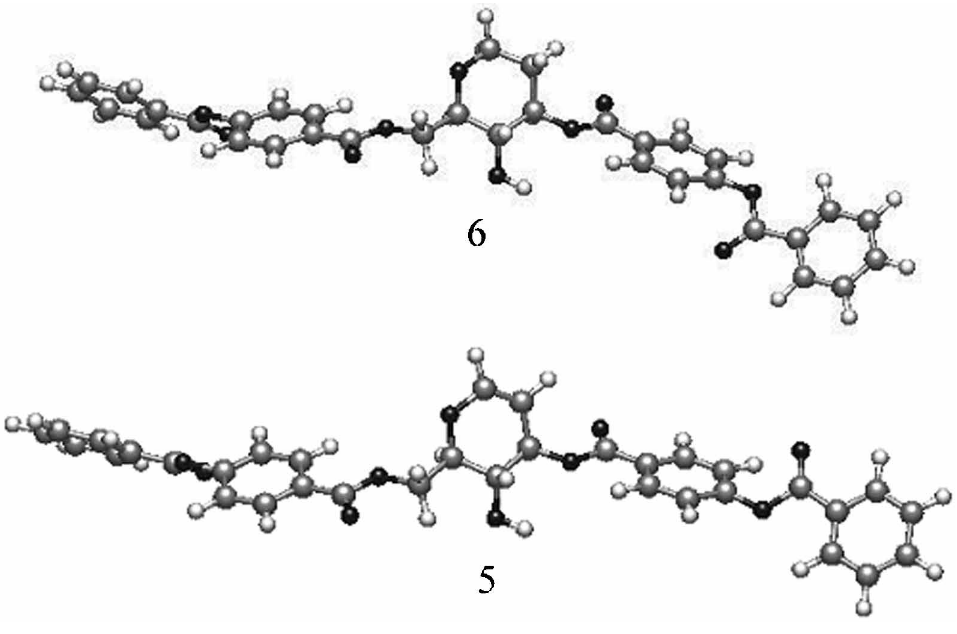

Figure 3. Simulation of molecular shapes of compounds **5** and **6**.

step, the double bond of compound **5** was hydrogenated using palladium on charcoal to give the desired compound **6**. Full details of synthesis are given in § 5.

The phase sequence of the resulting compound, on cooling, as determined by polarizing optical microscopy (POM) (Nikon OPTIPHOT2-POL, equipped with a Mettler FP52 hot stage) in sandwich cells is I 180 N* 140 Sm (B_X) 134 Cr (°C). The smectic (B_X) phase is monotropic and its transition can occasionally be supercooled by a few degrees.

The cholesteric pitch of the helical superstructure lies within the visible spectrum and was determined by the colour change method [7] in a $d=6\,\mu m$ commercial liquid crystal sandwich cell (E.H.C., Japan). The temperature dependence of the spontaneous polarization $\mathbf{P}_S$ of the smectic phase was determined by the well known triangular wave method [8] using the following parameters: cell gap $d=6\,\mu m$, electric field amplitude $\mathbf{E}=10\,MV\,m^{-1}$ and frequency $f=200\,Hz$. For larger field amplitudes electrohydrodynamic flow sets in. The dependence of $\mathbf{P}_S$ on the applied electric field amplitude was measured at the constant temperature $T=137°C$.

As the material cannot be uniformly oriented, the temperature dependence of the tilt angle θ had to be estimated from the switching angle 2θ of the Maltese cross observed in circular domains between crossed polarizers. During switching, no change in transmission was recorded, thus response times were determined from the current reversal peaks at applied square wave voltages using the conditions described already.

3. Experimental results and discussion

3.1. *Conformation*

There is a strong resemblance between the molecular shape of compounds **5** and in particular **6** with some typical banana-shaped molecules, for example the benzoic esters of resorcin. Therefore **5** and **6** can be considered as members of this class of molecules with a non-aromatic, chiral bent-core. The unsaturated compound **5** shows no mesogenic properties; it exhibits a melting point (the crystal to isotropic transition) at $T=163°C$ with no monotropic phases observed on cooling at different rates, as observed by POM. In contrast, compound **6** does exhibit liquid crystalline phases. Differing from typical bent-core mesogens, **6** is characterized by a torsion angle between the mesogenic side chains, due to the bent-core's chirality. The molecular geometry of compounds **5** and **6** is shown in figure 3.

The simulation of the molecular shapes was performed using the WinMOPAC V2.0 Molecular Orbital Program [9]. Calculations were carried out using the AM1[10] method and the EF [11] optimization procedure. The final gradient norm of the energy gradient was less then $0.05\,kcal\,mol^{-1}$. The structures gain some flexibility because of the CH_2 group attached to the alkyl ring; therefore these molecules can exhibit different rotamers. The simulations for the most favourable rotamers posses the *pro-R* (Re) hydrogen of the CH_2 group antiperiplanar to the neighbouring proton of the alkyl ring. Measurements of the torsion angle between the mesogenic side groups result in $-160°$ for compound **5** and $-147°$ for compound **6**.

3.2. *Mesogenic and physical properties*

On cooling from the isotropic melt, a typical cholesteric oily-streaks texture is observed, figure 4 (*a*), exhibiting a wavelength of selective reflexion $\lambda_0=\tilde{n}P$ in

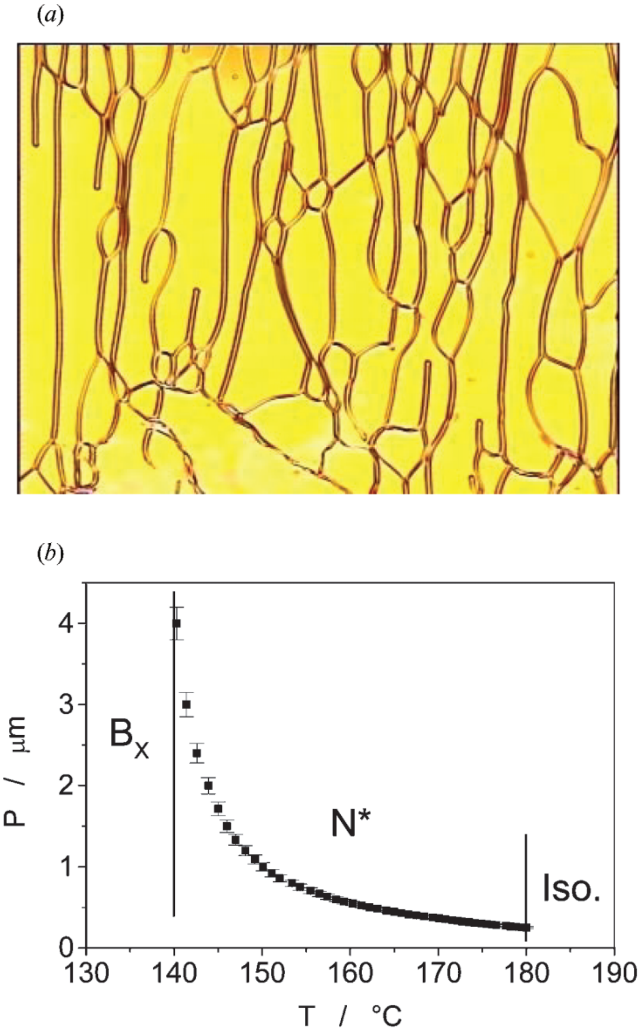

Figure 4. (*a*) Cholesteric oily-streaks texture, close to the transition to the smectic phase at $T=141°C$. The image size is $350\times280\,\mu m^2$. (*b*) Temperature dependence of the cholesteric pitch *P*. Positive values indicate a right-handed helical superstructure.

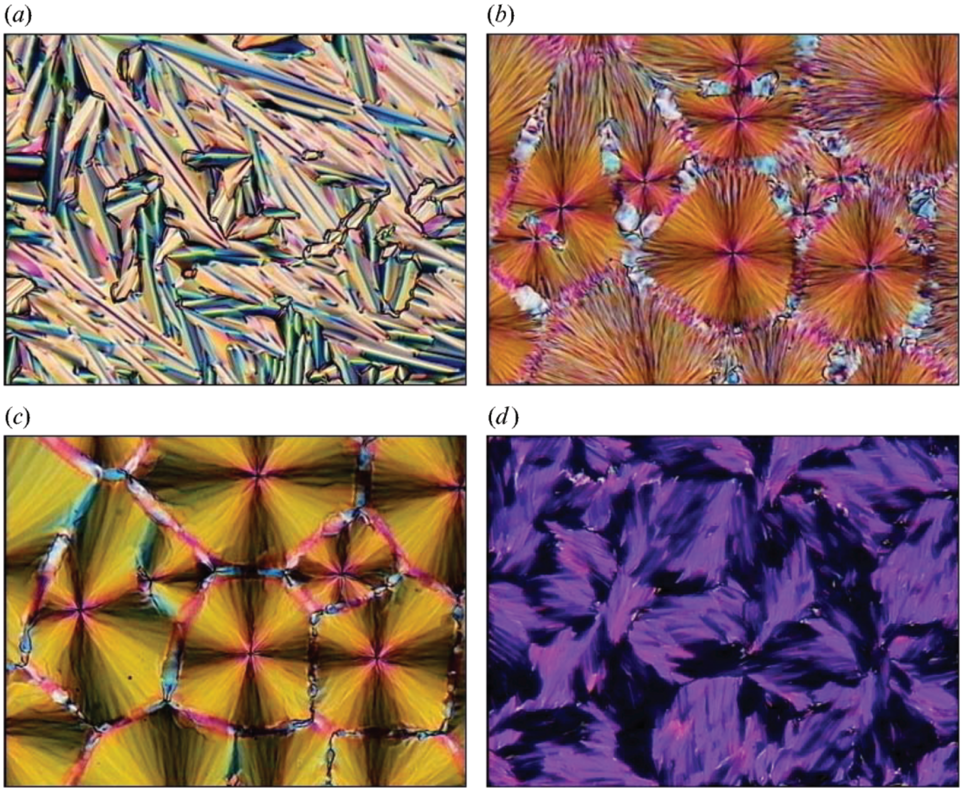

Figure 5. Series of texture micrographs in the smectic phase. (*a*) Virgin texture after cooling from the cholesteric phase; (*b*) circular domain formation and electrohydrodynamic flow at applied electric field of amplitude $\mathbf{E} = 15\,\mathrm{MV\,m^{-1}}$, $f = 200\,\mathrm{Hz}$; (*c*) corresponding texture at $\mathbf{E} = 10\,\mathrm{MV\,m^{-1}}$, $f = 200\,\mathrm{Hz}$, where ferroelectric/antiferroelectric switching is observed; (*d*) texture after decrease of the field amplitude to $\mathbf{E} = 0$ and $f = 1\,\mathrm{Hz}$. All images were taken at $\mathbf{T} = 135°\mathrm{C}$, with an image size of $350 \times 280\,\mu\mathrm{m}^2$.

the visible spectrum over a wide temperature range. Figure 4 (*b*) shows the corresponding temperature dependence of the cholesteric pitch *P*, assuming a reasonable value for the average refractive index of $\tilde{n} = 1.5$. The pitch decreases with increasing temperature, a behaviour commonly observed in calamitic cholesteric liquid crystals, with the helix being right-handed (positive pitch).

On cooling across the N* to smectic transition, a microscopic image similar to a fan-shaped texture of calamitic smectics is observed, figure 5 (*a*). The application of a moderate electric field ($\mathbf{E} < 5\,\mathrm{MV\,m^{-1}}$) indicates no ferroelectric switching. Further increase in electric field amplitude causes a slight change in birefringence, but still no switching. At field amplitudes $\mathbf{E} > 12\,\mathrm{MV\,m^{-1}}$ a dramatic texture reorientation is observed, accompanied by electrohydrodynamic flow and the formation of basically circular domains figure 5 (*b*). Subsequently, decreasing the field amplitude **E** diminishes the flow, figure 5 (*c*), and a switching process can be verified, until for $\mathbf{E} < 2\,\mathrm{MV\,m^{-1}}$ or for small frequencies $f < 20\,\mathrm{Hz}$ another texture reorientation occurs and switching again vanishes, figure 5 (*d*).

This behaviour is reflected in the current response for applied triangular waveforms as shown in figure 6. Before the high field treatment (solid line) only ohmic

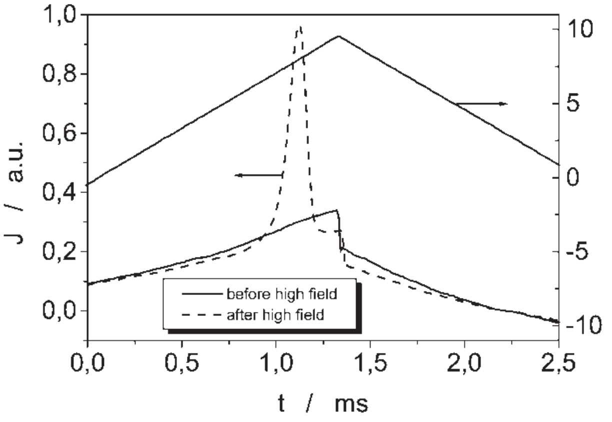

Figure 6. Current response before (solid line) and after (dashed line) the electric high field treatment, inducing circular domains. Before the field treatment, only ohmic and capacitive current contributions are observed, while after application of a large electric field, the current peak indicates ferroelectric/antiferroelectric switching.

and capacitive current contributions are observed. After induction of the circular domain texture, a peak in the current response indicates ferroelectric or antiferroelectric switching (dashed line). Even though two separate current peaks (as often observed for the antiferroelectric phase of calamitic molecules at low frequencies) could not be resolved, the high threshold field for switching indicates that the investigated banana phase exhibits antiferroelectric behaviour.

From integration of the current peak, a spontaneous polarization $\mathbf{P}_S$ is determined, which is dependent on the applied electric field amplitude, as shown in figure 7 (*a*). For $\mathbf{E} > 10\,\mathrm{MV\,m^{-1}}$ electrohydrodynamic flow sets in, which makes further determination of the polarization impossible. The temperature dependence of $\mathbf{P}_S$ is shown in figure 7 (*b*) for an applied electric field amplitude of $\mathbf{E} = 10\,\mathrm{MV\,m^{-1}}$. This shows the typical behaviour for a first order phase transition.

As the switching process within the mesogenic B_x phase is not accompanied by a change in transmission, no conventional electro-optic method can be used for the determination of the director tilt angle θ. The latter was estimated from the switching of the dark Maltese cross observed for domains of concentric, circular layer arrangement between crossed polarizers. For negative applied voltage, the cross switches clockwise, figure 8 (*a*). Reversal of the electric field direction causes a reorientation of the molecules, which can be observed macroscopically by a counter-clockwise rotation of the Maltese cross, as shown in figure 8 (*b*). We

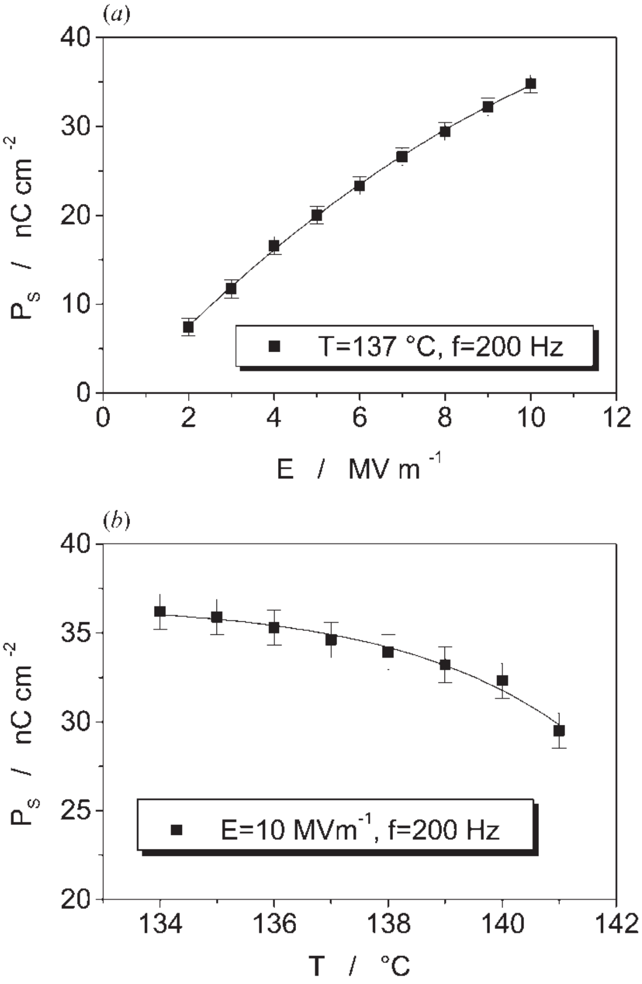

Figure 7. (*a*) Electric field dependence of the spontaneous polarization $\mathbf{P}_S$ at $T = 137°\mathrm{C}$. The decrease of the polarization for decreasing field is due to a gradual texture transition to that shown in figure 2 (*d*). (*b*) Temperature dependence of the spontaneous polarization at $\mathbf{E} = 10\,\mathrm{MV\,m^{-1}}$.

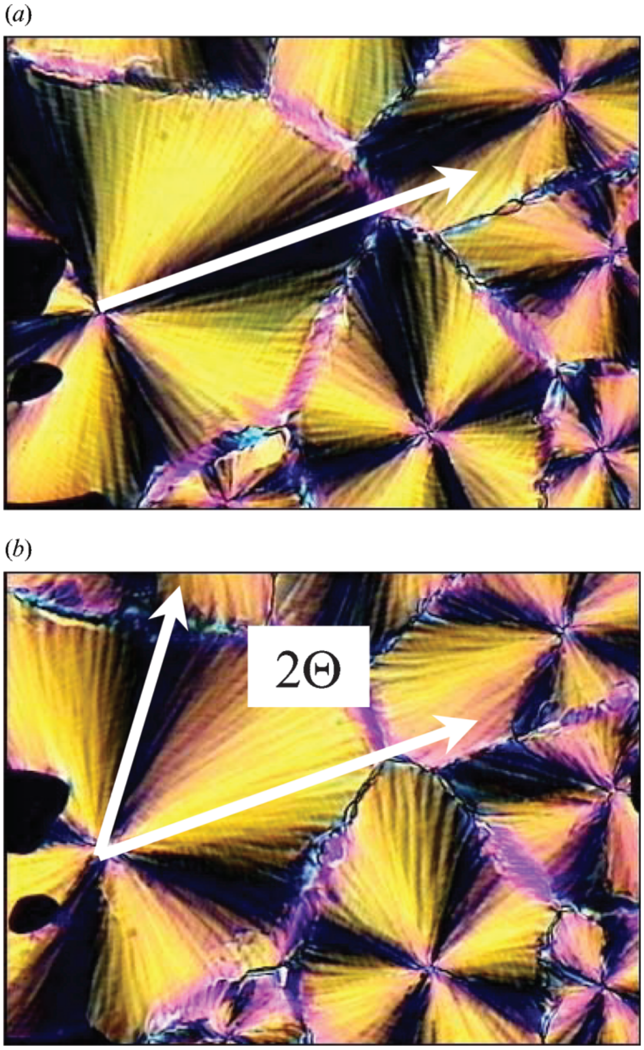

Figure 8. Two switching states of the circular domain texture at (*a*) negative and (*b*) positive electric fields. From the switching angle of the dark Maltese cross, the tilt angle θ can be estimated. Note that all domains switch in the same direction. The image size is $350 \times 280\,\mu\mathrm{m}^2$.

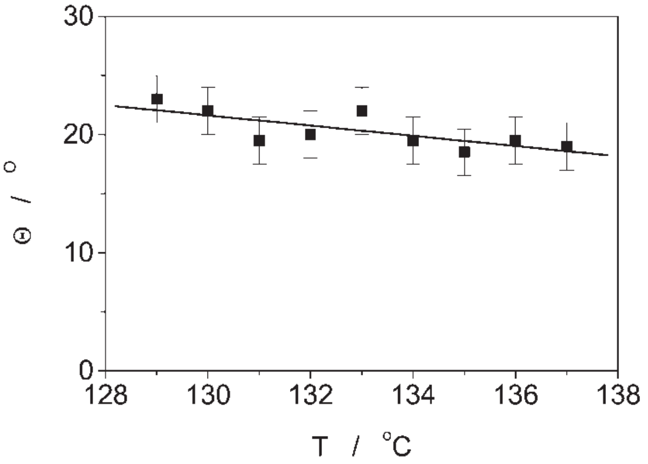

Figure 9. Temperature dependence of the tilt angle θ, as determined from the switching of the dark Maltese cross shown in figure 8.

note that all domains switch in the same direction. This is due to the chirality of the system introduced by the chirality of the bent-core mesogens, and is qualitatively different from switching in achiral banana phases. These may exhibit a spontaneous resolution of domains of opposite handedness, which then switch in an opposite fashion [12]. The temperature dependence of the tilt angle θ determined in this manner is shown in figure 9. An essentially constant tilt of approximately $\theta = 20^\circ$ is observed, which is the common behaviour found for first order phase transitions.

Generally, the response times τ of switching processes in liquid crystals are measured from the respective electro-optic transmission curves. This was impossible in the present case, as the switching process in the smectic phase was not accompanied by a change in transmission. Hence, τ was determined from the width of the current reversal peak (figure 6) and its temperature dependence is shown in figure 10. Switching times decrease strongly on increasing temperature, which can readily be attributed to a decrease in viscosity.

Estimation of the effective rotational viscosity γ from the relationship $\gamma = \tau \mathbf{P}_S \mathbf{E}$ for several temperatures gives reasonable values, figure 11 (*a*), and of the order of those observed for calamitic fluid smectics. An Arrhenius-plot, figure 11 (*b*), yields an activation energy of $E_a = 55\,\mathrm{kJ\,mol}^{-1}$, which is also in agreement with values observed for fluid smectics.

4. Conclusions

The synthesis, characterization and electro-optic properties of the first bent-core mesogen based on a chiral carbohydrate central bent are reported. It is shown that these materials can exhibit both traditional calamitic phases, as well as so called banana phases, typical for bent-core molecules. From texture observations and electro-optic experiments we conclude that

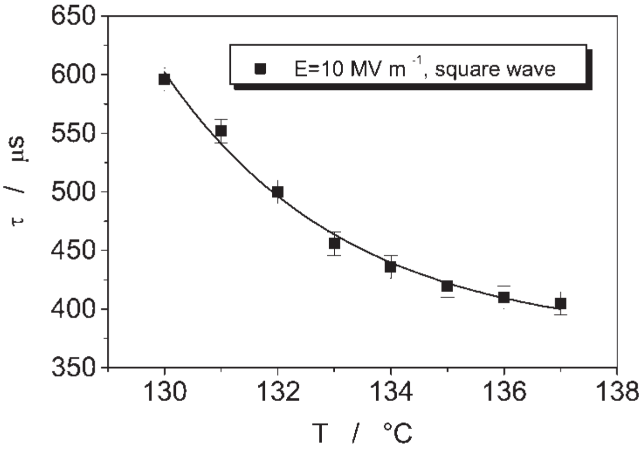

Figure 10. Temperature dependence of the switching time τ, determined from the current response to a $\mathbf{E} = 10\,\mathrm{MV\,m}^{-1}$ square wave electric field.

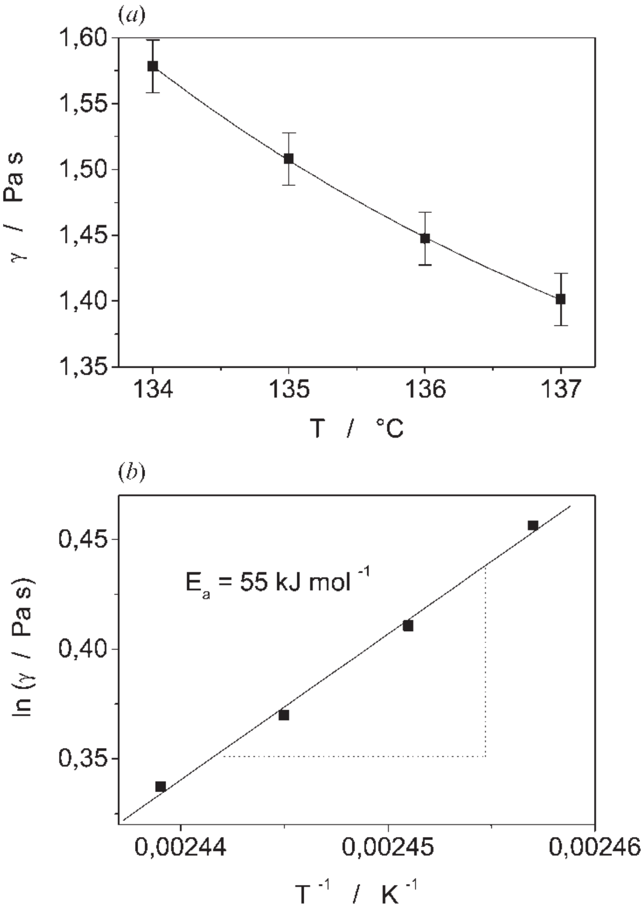

Figure 11. (*a*) Estimated temperature dependence of the effective rotational viscosity γ; (*b*) corresponding Arrhenius-plot, which yields an activation energy of $\mathbf{E}_a = 55\,\mathrm{kJ\,mol}^{-1}$.

the low temperature phase below the cholesteric phase of this compound is a fluid smectic, presumably a B_2 phase. It cannot definitely be excluded that the observed low temperature phase may have a different structure (B_1 or B_7), although texture observations do not support this conclusion. For a definite structural resolution X-ray investigations on oriented samples are needed, which are not available at present.

5. Synthesis details

5.1. *Characterization*

Thin layer chromatography was performed on silica gel (Merck GF245), and detection was effected by UV-absorbance and by spraying with a solution of ethanol/sulfuric acid (9/1), followed by heating. Column chromatography was performed on silica gel 60 (230–240 mesh, Merck). Optical rotations were recorded using a Perkin-Elmer PE 243 or 341 polarimeter. NMR spectra (1H: 400 MHz, 13C: 100.6 MHz) were recorded on a Bruker AMX-400 spectrometer with tetramethylsilane (TMS) as an internal standard. All optical rotation measurements were carried out using $CHCl_3$ unless specified. All reactions were carried out with dried solvents.

5.2. *D-Glucal, 2*

Commercially available compound **1** (10.00 g, 36.7 mmol) was dissolved in dry methanol (200 ml), sodium carbonate (10 g, 122 mmol) was added and the mixture stirred for 12 h at room temperature [13]. The mixture was filtered and the solvent removed under vacuum. The resulting crude product was used for the next conversion without further purification. Yield 4.56 g (syrup, 31.2 mmol, 85%); $[\alpha]_D^{20} = -11.7$ ($c = 0.8$, MeOH). ^{1}H NMR (400 MHz, CD_3OD): $\delta = 6.37$ (dd, 1H, H-1), 4.70 (dd, 1H, H-2), 4.14 (ddd, 1H, H-3), 3.90 (dd, 1H, H-6a), 3.81 (dd, 1H, H-6b), 3.74 (ddd, 1H, H-5), 3.59 (dd, 1H, H-4) ppm; $J_{1,2} = 5.1$, $J_{1,3} = 1.5$, $J_{2,3} = 2.0$, $J_{3,4} = 7.1$, $J_{4,5} = 9.7$, $J_{5,6a} = 2.5$, $J_{5,6b} = 5.1$, $J_{6a,6b} =$ 12.2 Hz. ^{13}C NMR (100 MHz, D_2O): $\delta = 144.13$ (C-1), 103.23 (C-2), 78.55 (C-5), 69.23, 68.70 (C-3, C-4), 60.47 (C-6) ppm.

5.3. *3,6-Di-*O*-(4-acetyloxybenzoyl)-D-glucal, 3*

Compound **2** (2.21 g, 15.1 mmol) was dissolved in 30 ml of a solution of dry dichloromethane and dry pyridine (1/1). A solution of 4-acetoxybenzoylchloride (6.16 g, 31 mmol) in 20 ml dry dichloromethane was then added slowly. The reaction was carried out under nitrogen, using catalytic amounts of 4-pyrrolidinopyridine. After completion of the reaction, the mixture was diluted with a small amount of dichloromethane, neutralized with 1M hydrochloric acid and washed with water. The organic phase was dried using magnesium sulphate. After filtration the solvent was removed under reduced pressure, and the crude product purified by column chromatography (petrolium ether (50–70)/ethyl acetate, 2/1). Yield 3.70 g (7.87 mmol, 52%) colourless crystals; $[\alpha]_D^{20} = -16.8$ ($c = 0.5$, $CHCl_3$); mp. 88.9°C. ^{1}H NMR (400 MHz, $CDCl_3$): $\delta = 8.09$, 8.06 (d, 2x 2H, H-2′Ar, H-6′Ar, H-2″Ar, H-6″Ar), 7.16, 7.15 (d, 2x 2H, H-3′Ar, H-5′Ar, H-3″Ar, H-5″Ar), 6.49 (d, 1H, H-1) 5.55 (ddd, 1H, H-3), 4.84 (dd, 1H, H-2), 4.81 (dd, 1H, H-6a), 4.63 (dd, 1H, H-6b), 4.17 (ddd, 1H, H-5), 4.01 (dd, 1H, H-4), 2.30 (s, 6H, 2x OAc) ppm; $J_{2'Ar,3'Ar} = J_{5'Ar,6'Ar} = 8.7$, $J_{2''Ar,3''Ar} = J_{5''Ar,6''Ar} = 8.7$, $J_{1,2} = 6.1$, $J_{1,3} = 1.0$, $J_{2,3} = 2.6$, $J_{3,4} = 6.6$, $J_{4,5} = 9.7$, $J_{5,6a} = 5.1$, $J_{5,6b} = 2.6$, $J_{6a,6b} = 12.2$ Hz. ^{13}C NMR (125 MHz, $CDCl_3$): $\delta = 169.14$ (2x Me$\underline{C}$OO) 166.29, 166.04 (2x Ar$\underline{C}$OO), 155.00 (C-4′Ar, C-4″Ar), 146.75 (C-1), 131.89, 131.87 (C-2′Ar, C-6′Ar, C-2″Ar, C-6″Ar), 128.39, 128.20 (C-1′Ar, C-1″Ar), 122.12 (C-3′Ar, C-5′Ar, C-3″Ar, C-5″Ar), 99.62 (C-2), 77.05, 73.96 (C-5, C-4), 67.78 (C-3), 63.30 (C-6), 21.30 (2x Me) ppm.

5.4. *3,6-Di-*O*-(4-hydroxybenzoyl)-D-glucal, 4*

Compound **3** (1.60 g, 3.40 mmol) was dissolved in 150 ml of dry methanol. A mixture of guanidinium hydrochloride (3.40 mmol) and sodium methanolate (160 mg, 2.96 mmol) in 50 ml dry methanol was then added. The reaction mixture was heated in a vacuum evaporator under low pressure (40°C, 270 mbar) to remove the solvent and methyl acetate. After drying, the crude product was dissolved in 1,2-dimethoxyethane. Hydrochloric acid was added and the mixture added slowly to 100 ml distilled water. The mixture was filtered and the residue dissolved in dichloromethane and dried using magnesium sulphate. After filtration the solvent was removed under reduced pressure. Yield 963 mg (2.49 mmol, 73%) colourless crystals; $[\alpha]_D^{20} = -54.2$ ($c = 0.6$, $CHCl_3$); m.p. 176.8°C. ^{1}H NMR (400 MHz, acetone-d_6): $\delta = 9.09$ (s, 2H, 2x OH), 7.81, 7.79 (d, 2x 2H, H-2′Ar, H-6′Ar, H-2″Ar, H-6″Ar), 6.79, 6.81 (d, 2x 2H, H-3′Ar, H-5′Ar, H-3″Ar, H-5″Ar), 6.40 (d, 1H, H-1) 5.39 (ddd, 1H, H-3), 4.99 (d, 1H, 4-OH), 4.74 (dd, 1H, H-2), 4.54 (dd, 1H, H-6a), 4.50 (dd, 1H, H-6b), 4.17 (ddd, 1H, H-5), 4.08 (mc, 1H, H-4) ppm; $J_{2'Ar,3'Ar} = J_{5'Ar,6'Ar} = 8.6$, $J_{2''Ar,3''Ar} = J_{5''Ar,6''Ar} = 8.6$, $J_{1,2} = 6.1$, $J_{1,3} = 1.0$, $J_{2,3} = 2.5$, $J_{3,4} = 6.7$, $J_{4\text{-}OH,4} = 5.1$, $J_{4,5} = 8.2$, $J_{5,6a} = 3.0$, $J_{5,6b} = 4.6$, $J_{6a,6b} = 12.2$ Hz. ^{13}C NMR (100 MHz, acetone-d_6): $\delta = 167.04$, 166.84 (2x COO), 163.18 (C-4′Ar, C-4″Ar), 146.84 (C-1), 133.04, 133.00 (C-2′Ar, C-6′Ar, C-2″Ar, C-6″Ar), 122.88, 122.70 (C-1′Ar, C-1″Ar), 116.49, 116.41 (C-3′Ar, C-5′Ar, C-3″Ar, C-5″Ar), 101.06 (C-2), 77.98, 73.34 (C-4, C-5), 67.71 (C-3), 63.85 (C-6) ppm.

5.5. *3,6-Di*-O-*[4-(4-octyloxybenzoyloxy)-benzoyl]*-D-*glucal,* **5**

Compound **4** (424 mg, 1.10 mmol) was dissolved in a solution of 150 ml of dry dichloromethane and 5 ml of dry pyridine. A solution of 4-octyloxybenzoylchloride (680 mg, 0.60 ml, 2.53 mmol) in 20 ml dry dichloromethane was then added slowly. The reaction was carried out using catalytic amounts of 4-pyrrolidinopyridine. After completion of the reaction, the mixture was diluted with a small amount of dichloromethane, neutralized with 1M hydrochloric acid and washed with water. The organic phase was dried over magnesium sulphate and the solvent removed under vacuum.

The crude product was recrystallized from ethanol/toluene (10/1). Yield 901 mg (1.06 mmol, 96%) colourless crystals; $[\alpha]_D^{20} = +6.5$ ($c = 0.5$, $CHCl_3$); m.p. 163°C. ^1H NMR (400 MHz, $CDCl_3$): $\delta = 8.18$–8.11 (m, 8H, H-2′Ar, H-6′Ar, H-2″Ar, H-6″, H-2‴Ar, H-6‴Ar, H-2⁗Ar, H-6⁗Ar), 7.33–7.29 (m, 4H, H-3′Ar, H-5′Ar, H-3‴Ar, H-5‴Ar), 6.98 (d, 4H, H-3″Ar, H-5″Ar, H-3⁗Ar, H-5⁗Ar), 6.54 (dd, 1H, H-1) 5.61 (ddd, 1H, H-3), 4.90 (dd, 1H, H-2), 4.86 (dd, 1H, H-6a), 4.69 (dd, 1H, H-6b), 4.23 (ddd, 1H, H-5), 4.08 (mc, 1H, H-4), 4.05 (t, 4H, 2x α-CH_2), 3.78 (d, 1H, 4-OH), 1.83 (mc, 4H, 2x β-CH_2), 1.48 (mc, 4H, 2x γ-CH_2), 1.39–1.19 (m, 16H, 8x CH_2), 0.90 (t, 6H, 2x Me) ppm; $J_{2''\mathrm{Ar},3''\mathrm{Ar}} = J_{5''\mathrm{Ar},6''\mathrm{Ar}} = 8.7$, $J_{2''''\mathrm{Ar},3''''\mathrm{Ar}} = J_{5''''\mathrm{Ar},6''''\mathrm{Ar}} = 8.7$, $J_{1,2} = 6.1$, $J_{1,3} = 1.0$, $J_{2,3} = 1.5$, $J_{3,4} = 6.6$, $J_{4\text{-OH},4} = 2.5$, $J_{4,5} = 9.7$, $J_{5,6a} = 4.6$, $J_{5,6b} = 2.5$, $J_{6a,6b} = 12.2$, $J_{\alpha\text{-H2},\beta\text{-CH2}} = 6.6$, $J_{\mathrm{CH2,CH3}} = 6.6$ Hz.

^{13}C NMR (125 MHz, $CDCl_3$): $\delta = 166.58$, 165.79, 163.88, 163.34 (4x COO, C-4″Ar, C-4⁗Ar), 154.85 (C-4′Ar, C-4‴Ar), 145.94 (C-1), 131.99, 131.09 (C-2′Ar, C-6′Ar, C-2″Ar, C-6″Ar, C-2‴Ar, C-6‴Ar, C-2⁗Ar, C-6⁗Ar), 127.58, 127.39 (C-1′Ar, C-1‴Ar), 121.55 (C-3′Ar, C-5′Ar, C-3‴Ar, C-5‴Ar), 120.57 (C-1″Ar, C-1⁗Ar), 113.99 (C-3″Ar, C-5″Ar, C-3⁗Ar, C-5⁗Ar), 98.87 (C-2), 76.85, 73.18 (C-5, C-4), 67.97 (2x α-CH_2), 67.01 (C-3), 62.53 (C-6), 31.38, 28.90, 28.80, 28.67, 25.57, 22.24 (12x CH_2), 13.67 (2x Me) ppm.

5.6. *3,6-Di*-O-*[4-(4-octyloxybenzoyloxy)-benzoyl]-1,5-anhydro-2-desoxy*-D-arabino-*hexitol,* **6**

Compound **5** (250 mg, 0.29 mmol) was dissolved in 40 ml ethyl acetate/ethanol (1/1). Catalyst Pd/C (5 mg, 10%) was added and the reaction mixture stirred under hydrogen at room temperature. After completion of the reaction the catalyst was filtered off and the solvent removed under vacuum. The crude product was recrystallized from ethanol/toluene (10/1). Yield 212 mg (0.25 mmol, 86%) colourless crystals; $[\alpha]_D^{20} = +39.4$ ($c = 0.5$, $CHCl_3$); **Cr** (140 SmX) 149.8 **Ch** 185.2 **I**. ^1H NMR (400 MHz, benzene-d_6): $\delta = 8.13$–8.05 (m, 8H, H-2′Ar, H-6′Ar, H-2″Ar, H-6″, H-2‴Ar, H-6‴Ar, H-2⁗Ar, H-6⁗Ar), 7.26–7.22 (m, 4H, H-3′Ar, H-5′Ar, H-3‴Ar, H-5‴Ar), 6.93–6.89 (m, 4H, H-3″Ar, H-5″Ar, H-3⁗Ar, H-5⁗Ar), 5.07 (ddd, 1H, H-3), 4.73 (dd, 1H, H-6a), 4.53 (dd, 1H, H-6b), 4.02 (mc, 1H, H-1_{eq}), 3.98 (t, 4H, 2x α-CH_2), 3.62 (dd, 1H, H-4), 3.55 (ddd, 1H, H-1_{ax}), 3.51 (ddd, 1H, H-5), 3.06 (bs, 1H, 4-OH), 2.14 (mc, 1H, H-2_{eq}), 1.84 (dddd, 1H, H-2_{ax}), 1.75 (mc, 4H, 2x β-CH_2), 1.40 (mc, 4H, 2x γ-CH_2), 1.34-1.20 (m, 16H, 8x CH_2), 0.84 (t, 6H, 2x Me) ppm; $J_{1ax,1eq} = 101.7$, $J_{1ax,2ax} = 11.7$, $J_{1ax,2eq} = 2.0$, $J_{1eq,2ax} = 4.6$, $J_{2ax,2eq} = 11.7$, $J_{2ax,3} = 11.7$, $J_{2eq,3} = 5.1$, $J_{3,4} = 9.1$, $J_{4,5} = 9.1$, $J_{5,6a} = 4.3$, $J_{5,6b} = 2.0$, $J_{6a,6b} = 12.2$, $J_{\alpha\text{-CH2},\beta\text{-CH2}} = 6.6$, $J_{\mathrm{CH2,CH3}} = 7.2$ Hz. ^{13}C NMR (125 MHz, $CDCl_3$): $\delta = 166.83$, 166.61, 164.73, 164.19 (4x COO, C-4″Ar, C-4⁗Ar), 155.49 (C-4′Ar, C-4‴Ar), 132.79, 131.94, 131.80 (C-2′Ar, C-6′Ar, C-2″Ar, C-6″Ar, C-2‴Ar, C-6‴Ar, C-2⁗Ar, C-6⁗Ar), 127.56 (C-1′Ar, C-1‴Ar), 122.31 (C-3′Ar, C-5′Ar, C-3‴Ar, C-5‴Ar), 121.40 (C-1″Ar, C-1⁗Ar), 114.79 (C-3″Ar, C-5″Ar, C-3⁗Ar, C-5⁗Ar), 79.55, 76.32 (C-5, C-4), 70.37 (C-3), 68.78 (2x α-CH_2), 65.99, 64.60 (C-1, C-6), 32.18, 31.49, 29.70, 29.60, 29.47, 26.37, 23.03 (C-2, 12x CH_2), 14.47 (2x Me) ppm.

References

[1] MEYER, R. B., LIEBERT, L., STRZELECKI, L., and KELLER, P., 1975, *J. Phys. Lett. (Paris)*, **36,** L69.

[2] NIORI, T., SEKENI, T., WATANABE, J., FURUKAWA, T., and TAKEZOE, H., 1996, *J. mater. Chem.*, **6,** 1231.

[3] PELZL, G., DIELE, S., and WEISSFLOG, W., 1999, *Adv. Mater.*, **11,** 707.

[4] LINK, D. R., NATALE, G., SHAO, R., MACLENNAN, J. E., CLARK, N. A., KÖRBLOVA, E., and WALBA, D. M., 1997, *Science*, **278,** 1924.

[5] BLACKBURNE, I. D., FREDERICKS, P. M., and GUTHRIE, R. D., 1976, *Aust. J. Chem.*, **29,** 381.

[6] KUNESCH, N., MIET, C., and POISSON, J., 1987, *Tetrahedron Lett.*, **31,** 3569.

[7] DIERKING, I., GIEßELMANN, F., and ZUGENMAIER, P., 1995, *Z. Naturforsch. A*, **50a,** 589.

[8] MIYASATO, K., ABE, S., TAKEZOE, H., FUKUDA, A., and KUZE, E., 1983, *Jpn. J. appl. Phys. Lett.*, **22,** L661.

[9] STEWART, J. J. P., and FUJITSU Limited, MOPAC97, Makuhari System Laboratory, 1-9-3 Nakase, Mihama-ku, Chib-shi, Chiba 261-8588, Japan.

[10] DEWAR, M. J. S., HEALY, E. F., HOLDER, A., and YUAN, Y.-C., 1990, *J. comput. Chem.*, **11,** 541.

[11] BAKER, J., 1986, *J. comput. Chem.*, **7,** 385.

[12] HEPPKE, G., JAKLI, A., RAUCH, S., and SAWADE, H., 1999, *Phys. Rev. E*, **60,** 5575.

[13] BERGMANN, M., and SCHOTTE, H., 1921, *Ber. Dtsch. Chem. Ges.*, **54,** 440.